THE ASTROPHYSICAL JOURNAL, 430:595–600, 1994 August 1

GALACTIC STRUCTURES ASSOCIATED WITH EXTREME SCATTERING EVENTS IN THE RADIO LIGHT CURVES OF NRAO 140, 0954+658, AND 2352+495

R. FIEDLER, T. PAULS, AND K. J. JOHNSTON
Remote Sensing Division, Naval Research Laboratory, Code 7200, Washington, DC 20375
AND
B. DENNISON
Center for Stochastic Processes in Science and Engineering, and Physics Department,
Virginia Polytechnic Institute and State University, Blacksburg, VA 24061
Received 1991 January 7; accepted 1994 January 28

ABSTRACT

Of the nine quasars whose radio light curves contain suspected extreme scattering events (ESEs), we find that the lines of sight toward three of them (NRAO 140, 0954+658, and 2352+495) pass through the edges of clearly identifiable Galactic structures seen at IR wavelengths and in 21 cm continuum emission. These structures are possible sites for enhanced turbulence in the electron column density distribution which, through diffractive or refractive propagation effects, may be responsible for the unusual flux density variations we denote as an ESE. Of the remaining six sources whose light curves display an ESE, four (0133+476, 0300+470, 1749+096, and 1821+107) appear near the edges of 100 μm IR clumps in the Galactic foreground and two (1502+106 and 1611+343) are 1°–2° from the nearest clump. We suggest that the shell-like object, observed in projection against NRAO 140, may be a very old nova remnant.

Subject headings: ISM: structure — quasars: general — radio continuum: galaxies — turbulence

1. INTRODUCTION

Extreme scattering events (ESEs) were first noticed in the 2.7 GHz light curves of 0954+658, 1502+106, and 1611+343 (Fiedler et al. 1987). The flux density variations that define an ESE may be characterized as a sequence of smooth variations usually possessing a large degree of symmetry about the midpoint of the event and having no resemblance to the variations normally observed in a given source. For example, the event at 2.7 GHz in 0954+658 comprises two week-long maxima that bracket a prolonged 8 week flat-bottomed minimum. A likely explanation for these unusual variations is that a region of enhanced turbulence in the electron density distribution local to our Galaxy passed through the line of sight to this quasar. Radio-wave diffraction and refraction through such a region having an angular extent comparable to the background source, could reproduce the kinds of variations observed in an ESE (see Fiedler et al. 1994).

The purpose of this paper is to present all clearly recognizable Galactic structures that appear in the foreground of sources whose light curves contain an ESE and to suggest that these structures represent potential sites of enhanced electron density fluctuations. Three such structures were found in the Galactic foreground to NRAO 140, 0954+658, and 2352+495. The structures all appear to be tracers of some form of Galactic outflow. We concentrate most of our efforts in this paper on the field associated with NRAO 140. Thus far, ESEs have been found in the light curves of nine quasars (Fiedler et al. 1994).

The Galactic fields in the foreground of the remaining six quasars may be categorized as clumpy. The IR and H I continuum foreground emission do not contain easily identifiable structures, but rather irregularly shaped clumps of emission. Four of the six quasars (0133+476, 0300+470, 1749+096, and 1821+107) are seen through the edges of foreground clumps and the remaining two (1502+106 and 1611+343) are 1°–2° from the nearest clump. The latter two sources are at roughly 50° north Galactic latitude and bracket the North Polar Spur.

Although we are unable to provide a direct connection between ESEs and the foreground Galactic structures presented below, the association is intriguing and certainly merits close examination. See Fiedler et al. (1994) for the light curves of the sources discussed here.

2. DISCUSSION

Associating ESEs with regions of apparent outflow in the Galaxy necessarily assumes a causal link between size scales in the ISM that span many orders of magnitude. Whereas the Galactic features presented here span many degrees, the angular extent of ESE-producing structures, estimated in Fiedler et al. (1987), is probably on the order of a milliarcsecond (mas). Romani (1988) has suggested that ESEs may be associated with large radio continuum loops that are believed to be old remnants of energetic supernovae, or collective superbubbles blown out by closely spaced supernovae (McCray 1987). Postshock gas at the edge of the expanding loop may produce the electron density distribution required for an ESE. The four well-known continuum loops in the Galaxy (Berkhuijsen, Haslam, & Salter 1971) represent possible sites for extreme scattering and have been correlated with the data obtained by our monitoring program for ESEs (Fiedler et al. 1994).

Although we find that the proposed association between ESEs and large loops appears to be qualitatively consistent with our small sample of events, we point out that ESEs have so far been observed to group in two areas of the sky. These areas correspond to the North Polar Spur and an area near the Galactic anticenter approximately 15° below the plane. This

grouping in the spatial distribution of ESEs could be a consequence of the poor statistics associated with our small sample, or could be a tracer of turbulent structures within the loops.

Even if Galactic loops are found to form the primary locus for ESE-producing regions, it should be noted that secondary phenomena induced by the outflow may be as important in producing an ESE as the shock front associated with the outflow itself. Induced star formation leading to large-scale stellar winds from OB associations, nova and supernova events, and possibly even ISM turbulence induced by the dynamic interaction of a pulsar magnetosphere with the surrounding medium are all potential sites for extreme radio propagation effects and ESEs. The conditions that are evidently needed to produce an ESE are a long path length relative to the width of the ESE structure and a source size which is comparable to the angular extent of the foreground region of enhanced turbulence in the electron density distribution.

We find that there is a significant correlation between the large-scale Galactic continuum loops and the lines of sight to quasars having an ESE in their radio light curve (Fig. 4 in Fiedler et al. 1994). However, identifying specific small-scale structures that may be directly responsible for ESEs is complicated by confused Galactic fields at the few degree scale size. Only three of the nine ESE sources have clearly defined foreground Galactic structures. The remaining six quasars (0133+476, 0300+470, 1502+106, 1611+343, 1749+096, and 1821+107) have lines of sight through either confused, or apparently empty, regions of the Galaxy. An examination of the available 21 cm H I line surveys will help to simplify the confused fields in the Galactic foreground of some of these six event sources.

The surveys we used to look for foreground Galactic structure were the Palomar Sky Survey, the *IRAS* survey, the Dwarakanath & Shankar (1990) 34.5 MHz survey, the Haslam et al. (1982) 408 MHz Survey, the Condon & Broderick (1985) 1400 MHz survey, and the Condon, Broderick, & Seielstad (1989) 4.85 GHz survey.

The fields surrounding each of the three sources discussed in this paper (NRAO 140, 0954+658, and 2352+495) are presented in Figures 1, 2, and 3 at low and high resolution. We give a large field of view, low-resolution (2° beam), 21 cm continuum map (Stark et al. 1981) (panel *a* of each figure) and a small field of view, higher resolution (4′ beam), *IRAS* map (panel *b* of each figure).

2.1. NRAO 140 ($l \simeq 158°, b \simeq -18°.8$)

As was mentioned earlier, there may be a causal link between Galactic structures that differ in size by many orders of magnitude, leading ultimately to the roughly AU-sized component responsible for an ESE. For this reason we attempt an understanding of the circumstances leading to ESEs using a top-down approach, i.e., progressing from large to small scale size. We conclude this section on NRAO 140 with the suggestion that two separate structures, associated with an outflow, produced the two ESEs observed in its 2.7 GHz light curve.

2.1.1. *Possible Galactic Associations*

The discussion that follows is motivated by the observation that the *IRAS* IR field adjacent to NRAO 140 contains a ring of knots that form a shell-like region approximately 1°.2 in diameter. NRAO 140 lies near the northwestern edge of this shell. The IR shell was first noticed by Pauls & Schwartz (1989) during their search of the *IRAS* database for extended objects to study in the CO (1–0) line. They found that little CO is associated with this shell, but suggest that the shell might be a supernova remnant. We will remark on this possibility later. There is no evidence for an optical counterpart in the Palomar Sky Survey, but the *IRAS* and the radio frequency surveys listed above show this region to be very complicated.

At the largest scale, we find that the Galactic foreground to NRAO 140 is located on the periphery of one of the continuum loops mentioned earlier, specifically Loop II. From an examination of the Colomb, Pflppel, & Heiles (1980) H I survey, the Galactic emission from this part of the sky is dominated by two closely spaced spurs extending below the Galactic plane. A hole in 21 cm emission separates the two spurs and, as is illustrated in Figure 1*a*, the line of sight to NRAO 140 passes through the smaller spur near the boundary of the hole. A similar, but less well defined, hole in the surface brightness distribution is also present in the IR.

Reducing our field of view further, we find that the IR shell appears to be embedded in the eastern half of the Perseus cloud complex. A visual extinction map of this region from Bachiller & Cernicharo (1986) shows the cloud complex to span 6° × 3°, with the long axis oriented to the northeast. Also, a band of local maxima in extinction and ^{13}CO emission overlaps the southeastern portion of the shell. The shell is bordered on the east by the molecular cloud IC 348 (e.g., Bachiller, Guilloteau, & Kahane 1987) and to the northeast and southwest by chains of young stellar objects and reflection nebulae. There is no evidence for young stellar objects within the shell itself.

Distance estimates to the Perseus cloud complex are still uncertain, but Cernicharo, Bachiller, & Duvert (1985) conclude that there are two layers of obscuring matter at 200 and 300 pc from the Sun. The larger distance, they believe, is probably the site for the Per OB2 association. The brightest stars of this stellar association lie to the northeast of the IR shell.

Sancisi et al. (1974) have modeled the kinematics of the Perseus cloud complex based on H I, OH, and CH line observations. They suggested that the cloud complex is a section of a much larger outflow, expanding at a velocity of 5 km s^{-1}, and that the Per OB2 association formed within that outflow roughly 1.5 × 10^6 yr ago (Blaauw 1964; Lesh 1969). They estimate the center of expansion to lie in the direction of $l = 160°$ and $b = -17°$.

Clearly, the region surrounding the IR shell is highly complex. Kinematic and statistical studies as well as the morphology indicated by H I surveys and the *IRAS* survey strongly suggest that this is a very active region.

We conclude our brief survey in scale size with an examination of the field interior to the shell. This field is particularly important as it has a bearing on the classification of the shell. The gigahertz frequency emission is dominated by a steep spectrum source NRAO 143 (3C92) that has no optical counterpart in the Palomar Sky Survey (see Fig. 1*b*). Preliminary results from 5 GHz VLA observations show this source to be double and with a peak polarization of roughly 12%. Riley (1989) has observed 3C92 at 2.7 GHz with the MRAO 5 km array in total intensity and were unable to find any optical counterpart.

The IR knot nearest to NRAO 143 is approximately 12′ to the south (see Fig. 1*b*). Interestingly, this knot is coincident with a 37 Jy feature at 34.5 MHz (Dwarakanath & Shankar 1990) indicating the presence of a nonthermal source. The positional accuracy of the low-frequency feature is estimated to be roughly 5′ and is therefore unlikely to be associated with

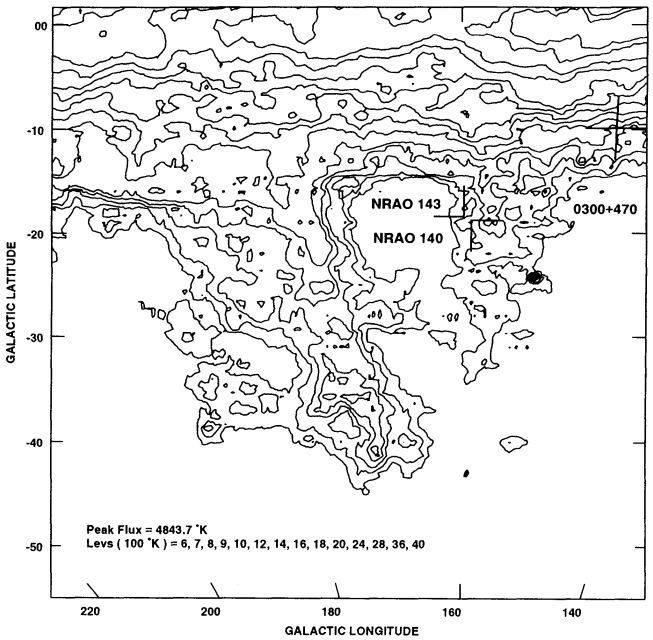

FIG. 1*a*

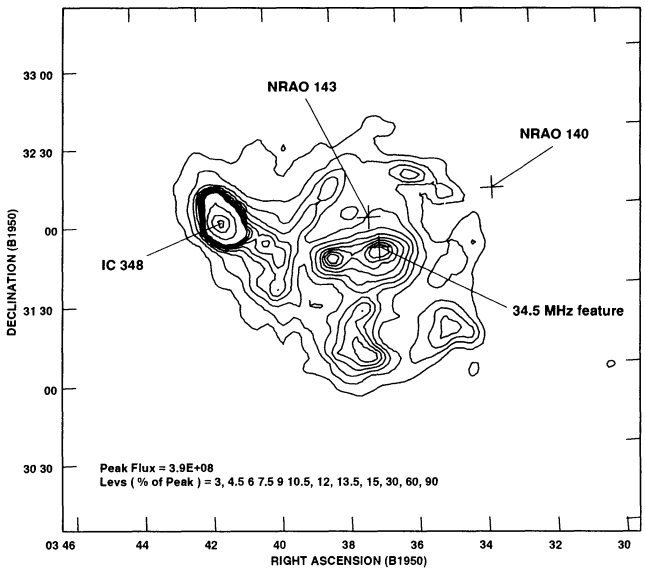

FIG. 1*b*

FIG. 1.—(*a*) Contour map in 21 cm continuum, for the field surrounding NRAO 140. This field includes 0300+471, a quasar whose 2.7 GHz light curve also contains an ESE. Panel (*a*) of all figures in this paper are based on the Bell Labs H I survey (Stark et al. 1981) and were taken from an all-sky continuum map created by Désert, Bazell, & Boulanger (1988). (*b*) A more detailed *IRAS* map, at 60 μm, illustrates the relative positions of NRAO 140 and a ring of IR knots immediately to the southeast. The little-known source NRAO 143 is probably a background extragalactic object. The cross to the south of NRAO 143 indicates the position of a 34.5 MHz 37 Jy feature that is coincident with an IR knot located near the centroid of the ring of knots.

NRAO 143. Although the exact nature of these two radio sources is uncertain, NRAO 143 is probably an unrelated background source, while the nonthermal feature coincident with the centrally located IR knot may be physically associated with the shell.

2.1.2. *Possible Causes for the IR Shell near* NRAO 140

The knots that define the IR shell may be the result of an interaction between an outflow and the surrounding ISM. In support of this possibility is the circular distribution of knots, where ridges in IR emission connect adjacent knots, and a centrally located nonthermal object that could be a compact remnant. As was pointed out, the gigahertz frequency emission from the shell is dominated by NRAO 143, which is probably an unrelated background source. This makes a comparison of IR and radio flux densities untenable for the purposes of directly assessing whether the shell itself is nonthermal. Higher resolution radio observations than that of the surveys used in our study are needed to clearly distinguish between the different sources of emission. For the present discussion, we assume that the shell is physically associated with the Perseus cloud complex at a distance of 250 pc. At this distance the 1°.2 diameter shell has a linear size of 5.2 pc.

We now consider the possibility that the shell is a supernova remnant (SNR). An assumed expansion velocity of 10,000 km s^{-1} implies an age for the remnant of 250 yr. This would put the SNR candidate in the same age class as the Cas A, Tycho, and Kepler SNRs. These SNRs are considered young and have 10–100 μm spectra that peak around 50 μm. The infrared spectrum of the shell, uncorrupted by suspected H II features (knots) and based on the plateau of emission west of the centroid, increases monotonically toward 100 μm. This is typical of much older SNRs. In addition, a young SNR might also be expected to be bright at X-ray wavelengths. However, the *HEAO* A-1 X-ray source catalog (Wood et al. 1984) shows a weak source centered roughly 10′ west of the shell, with a 0°.25 × 2°.25 east-west error box. If the X-ray flux originates within the shell, we find that the X-ray brightness of the shell is at least two orders of magnitude less than that for the young SNRs mentioned above. These comments raise the possibility that the shell, if it is a SNR, may be at a distance much greater than 250 pc and, therefore, totally unrelated to the Perseus cloud complex.

A lower energy event, such as a nova explosion, appears to be more consistent with the 250 pc distance estimate. However, the expansion age of the shell, on the order of 2500 yr, would make the shell the oldest recognized nova remnant. The expansion age is derived from an assumed outflow speed of 1000 km s^{-1}.

We find it unlikely that the shell is the result of a stellar bubble. This follows from a comparison of the estimated expansion age of the shell, less than 3×10^5 yr, and the expected lifetime of a shell produced by an OB association or a Wolf-Rayet star, 10^6 yr. One would expect to find young stellar objects within the field of the shell, but none appear to be present (Bachiller & Cernicharo 1986). In estimating the expansion age, we assumed a very small lower limit for the average expansion velocity, 10 km s^{-1}. See, for example, Weaver et al. (1977) and van Buren & McCray (1988).

2.1.3. *Two ESEs in the* 2.7 GHz *Light Curve*

In this section we shall use the duration and timing between events, in concert with the milliarcsecond morphology of NRAO 140, to make some simple statements about the struc-

tures responsible for the ESEs observed in the radio light curve of this source. The milliarcsecond structure of NRAO 140 has been observed to be complex and shows evidence for superluminal motion (Marscher & Broderick 1982, 1985). The 1984 6 cm VLBI observation of this source by Marscher et al. (1987) shows five, and possibly six, components in a linear jet spanning approximately 10 mas. Surprisingly, the jet orientation (P.A. $\simeq$ 130°) is within 10° of the line connecting the centroid of the shell and NRAO 140 (P.A. $\simeq$ 138°). If the shell is associated with an outflow of material, the outflow should transit all of the components in succession.

From Marscher et al. (1987), a decomposition of the total radio spectrum into spectra of the individual components indicates that at 2.7 GHz the brightest components are *B* and *E* with flux densities of 1.4 and 0.5 Jy, respectively. The outflow discussed above would propagate from components *E* to *B*. These components are roughly 7 mas apart and appear not to have varied appreciably in separation, or intensity, between the 6 cm VLBI observations of NRAO 140 in 1981 August and 1984 May. We note that the ESEs occurred in 1986 May and 1987 December, separated in time by 582 days or 1.6 yr.

The direction of proper motion of an object in the Perseus cloud complex due to solar motion, Earth orbital motion, and differential Galactic rotation is roughly aligned along the axis joining the radio components of NRAO 140. However, the extent of the proper motion for the time interval between the ESEs is approximately 3 times the separation between components *B* and *E*. A single structure could not have produced the events by passing through the foreground of the two components in succession. Moreover, including a peculiar proper motion for the structure corresponding to radial outflow results in a misalignment with the axis of the radio components for an outflow velocity greater than a few kilometers per second.

From the estimated surface density of ESEs, less than 450 arcsec^{-2} (Fiedler et al. 1994), we find that two separate structures passing through the line of sight to NRAO 140 is not unreasonable. Assuming a distance of 250 pc to the structures and using the time interval between the two events, 582 days, we infer a relative transverse velocity of 35 km s^{-1}.

We suggest that the differences in duration, depth, and time between the two events result from slightly different sizes and density fluctuations in two structures that transited the dominant 2.7 GHz component in NRAO 140. Variations due to the remaining components are not likely to be distinguishable from the level of the persistent fluctuations seen in the 2.7 GHz light curve of NRAO 140, since the second brightest component is fainter by a factor of 3 (Marscher et al. 1987).

2.2. 0954+658 ($l \simeq 145\overset{\circ}{.}7, b \simeq 43\overset{\circ}{.}1$)

The edge of Galactic Loop III (Berkhuijsen et al. 1971) is seen in projection against 0954+658. Loop III extends from the Galactic background near $l = 125°$, $b = 30°$ northward to $l = 135°$, $b = 40°$ and merges with the background near $l = 155°$, $b = 30°$ (see Fig. 2*a*). The position of 0954+658 is indicated by the cross. This loop and the other three large-scale Galactic loops are each believed to be the result of one or more supernova explosions. In support of this, Heiles & Jenkins (1976) have argued that H I filaments associated with Loop III are consistent with a dense region located behind a shock front having small-scale structure that is compatible with supersonic turbulence.

Hu (1981), in this study of high-latitude H I shells, subdivides this loop into one main shell, roughly 10° in diameter, and two subshells, each roughly 4° in diameter. The shells are identified in Table 1 of Hu as shells numbered 26, 26a, and 26b. The edge of subshell 26b, appearing as an extension above the main loop, overlaps the sky position of 0954+658. This subshell is

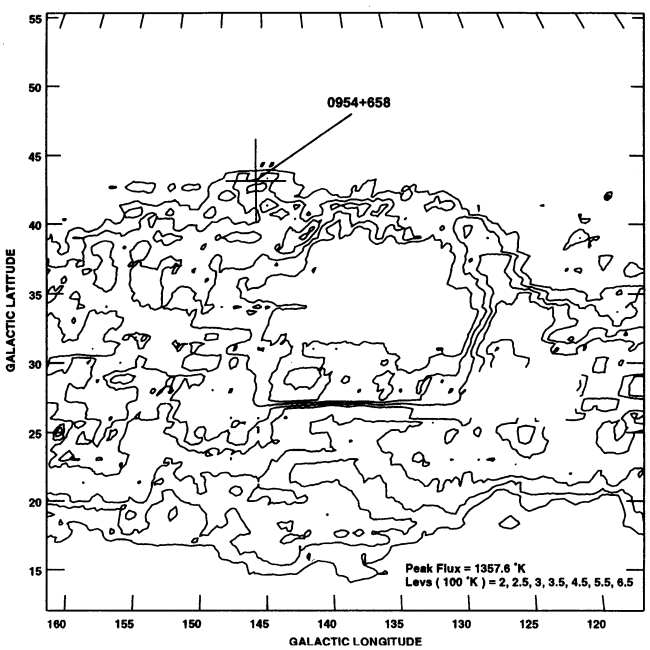

FIG. 2*a*

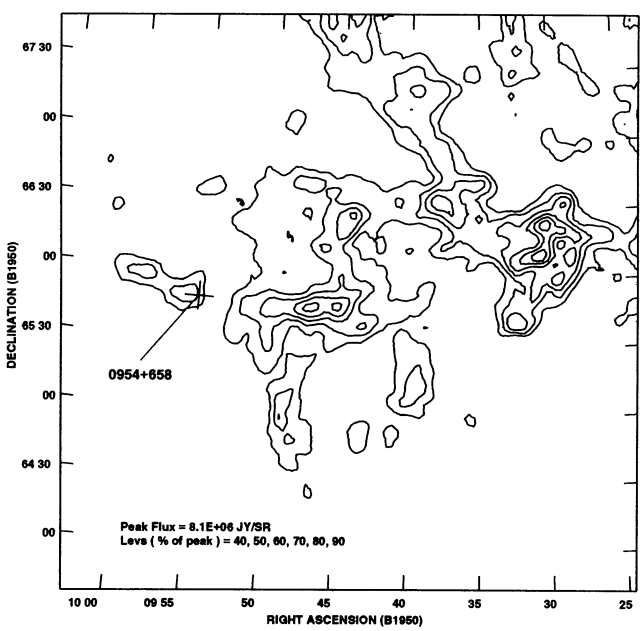

FIG. 2*b*

FIG. 2.—(*a*) Contour map in 21 cm continuum, for the field surrounding the quasar 0954+658. This quasar is seen through the northeastern edge of Galactic Loop III. (*b*) A higher resolution 100 μm *IRAS* map, for a smaller field surrounding 0954+658. The irregular morphology of the IR structure near 0954+658 suggests that the ESE in this source was produced by turbulence in the electron density distribution from fragments of the large-scale loop structure (*a*).

estimated by Hu to be at a distance of 145 pc with an average H I number density on the order of 10 cm^{-3}. Figure 2*b* shows a detailed view of the loop near 0954+658.

2.2.1. *The ESE in the* 2.7 GHz *Light Curve*

We interpret the H I shell and associated subshells as structures that border probable sites for small-scale inhomogeneities in the electron density distribution. An examination of all of the foreground fields surrounding the nine ESE quasars shows the quasars to lie in the periphery, rather than in the center, of H I and IR features. We suggest that one of the inhomogeneities was responsible for the ESE in 0954+658. We can use the estimated distance to the foreground subshell to refine our earlier estimate of the scale size of the structure and its inhomogeneities (Fiedler et al. 1987). Using an estimated angular size for 0954+658 of about 1 mas at 2.7 GHz, the proper motion of the structure is estimated to be about 0.09 mas per day. At a distance of 145 pc, the structure would have an overall size of about 0.6 AU, with the inhomogeneities on scales about one-tenth this size. The overall size is estimated from the duration of the event, and the inhomogeneity scale is estimated from the sharp focusing spikes observed at 8.1 GHz. The resulting transverse velocity is about 20 km s^{-1}.

Such a small transverse velocity suggests that the Earth's orbital motion may have some effect on the shape of the ESE, especially in the 2.7 GHz light curve. As suggested in Fiedler et al. (1987), the changing transverse velocity of the Earth during an event could effectively distort the temporal scale and possibly account for the observed difference in widths of the bracketing maxima. In this case, the Earth's motion was approximately normal to the observers' line of sight toward 0954+658 during the early part of the event, and roughly along the line of sight near the end. The ecliptic latitude of 0954+658 is 48°. Of course, asymmetric properties associated with the structure itself could easily dominate the shape of the light curve.

2.3. 2352+495 ($l \simeq 114°, b \simeq -12°$)

The Galactic foreground of this source, like 0954+658, is also coincident with the large-scale Galactic continuum Loop III, but is located at the opposite side of the loop from 0954+658. A large-scale 21 cm continuum map is shown for this region in Figure 3*a*, where 2352+495 is indicated by the cross. The southern extreme of Loop III is parallel to the plane of the Galaxy and is therefore difficult to distinguish from the continuum disk emission.

Although the detailed Galactic foreground to 2352+495 at 100 μm does not show any loop or shell-like structures, the line of sight to this quasar passes close to an IR knot whose morphology is somewhat reminiscent of the head-tail geometry of radio jets observed in some clusters of galaxies (see Fig. 3*b*). This analogy implies a substantial relative motion between the knot and the surrounding ISM, sufficient for ablation or internal ejection mechanisms to cause material to become heated and swept back away from the direction of motion.

We point out that this knot appears in a string of knots that spans approximately 3°. The Catalog of Infrared Observations (Gerazi, Schmitz, & Mead 1987), which is based on the *IRAS* survey, lists only two IR point sources inside the field plotted in Figure 3*b*. One of them is the star R Cas (IRAS 23558+5106), located at the top of the figure, and the other is RAFGL 5797S located between the tails of the IR knot near 2352+495 (see Fig. 3*b*).

If the ESE in this source is associated with the IR knot, then the ESE was probably due to a passing shock front. We emphasize, however, that the presumed motion of the IR knot

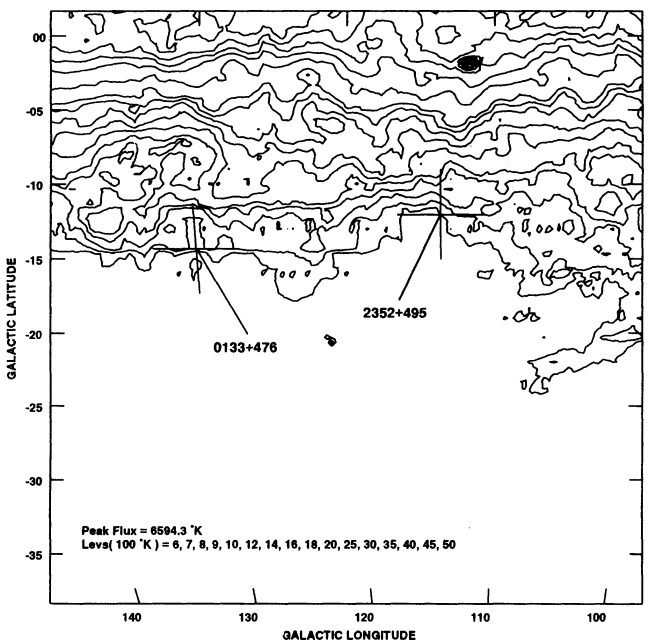

FIG. 3*a*

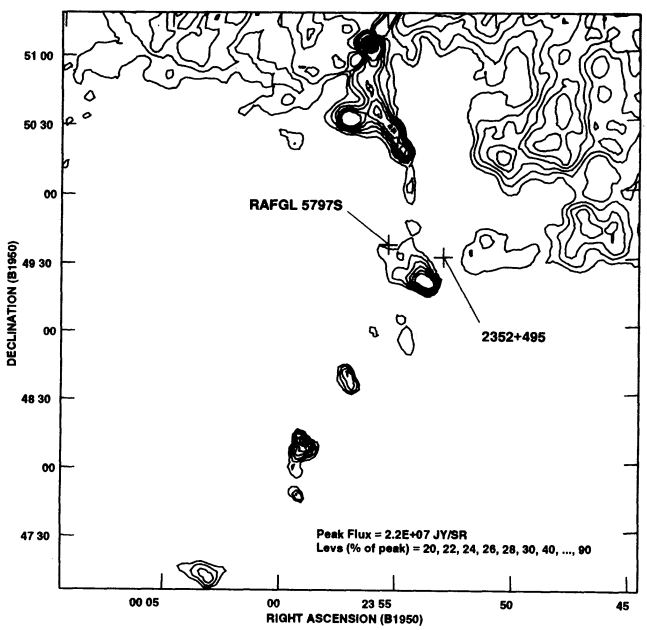

FIG. 3*b*

FIG. 3.—(*a*) Contour map in 21 cm continuum, for the field surrounding the quasar 2352+495. This field includes 0133+476, a quasar whose 2.7 GHz light curve also contains an ESE. (*b*) A higher resolution 100 μm *IRAS* map, for a smaller field surrounding 2352+495. The 2 μm IR point source RAFGL 5797S is seen between the tails of the IR knot near the quasar. The head-tail morphology of the knot is suggestive of motion through the local ISM, which may be sufficient to create enough turbulence to produce an ESE in the light curve of 2352+495. It is not known whether the point source is physically associated with the IR knot.

is speculation and is based solely on the knot morphology. Detailed observations of this knot may help to resolve whether its relative motion through the local ISM is sufficient to produce the extended infrared emission properties illustrated in Figure 3*b*.

3. CONCLUSIONS

The Galactic foregrounds to NRAO 140, 0954+658, and 2352+495 provide the best examples of a possible association between ESEs and specific Galactic structures. The foreground structures presented here have morphologies that are consistent with motion through the ISM, where shocks, and therefore electron density distributions and turbulence, may be present. Long path lengths through the limbs of these structures, combined with enhanced turbulence, may be necessary for an ESE to occur, provided that there is a background source of angular extent comparable to the foreground structure.

The three quasars, and indeed nearly all of the sources that display an ESE in their radio light curves, are seen through one of the four well-known large-scale continuum loops seen in the Galaxy. These loops are generally believed to be the result of either single, or multiple, supernova explosions (e.g., Berkhuijsen et al. 1971; McCray 1987). The turbulence and extended path lengths that may be attributed to shock fronts due to either the loops themselves or to secondary effects, such as star formation and subsequent evolution toward cataclysmic events, are potential sites for ESE-producing structures. The small-scale Galactic foreground to NRAO 140 (Fig. 1*b*) and 2352+495 (Fig. 3*b*) appear to be secondary structures induced by the passage of the larger scale Galactic loop. Conversely, the highly irregular appearance of the foreground to 0954+658 (Fig. 2*b*), suggests that the material responsible for the ESE in this source may be due to filaments, or segments, of the shock associated with the expanding loop itself.

The nature of the ring of IR knots near the line of sight to NRAO 140 is unclear, but detailed observations of NRAO 143 and the IR knots themselves will hopefully reveal the origin of this shell-like region. If the shell is at the distance of the Perseus cloud complex, then the shell may be a very old nova remnant that is recognizable by virtue of its high Galactic latitude.

The six quasars not discussed in this paper (0133+476, 0300+470, 1502+106, 1611+343, 1749+096, and 1821+107), all having an ESE in their radio light curve, have either confused or apparently empty Galactic foreground fields, based on the *IRAS* survey and 21 cm continuum emission. Possible associations with Galactic structure will be sought along these lines of sight using the velocity discrimination of 21 cm line surveys.

The authors are grateful to Jim Cordes and Andrew Clegg for comments on the manuscript.

REFERENCES

Bachiller, R., & Cernicharo, J. 1986, A&A, 166, 283
Bachiller, R., Guilloteau, S., & Kahane, C. 1987, A&A, 173, 324
Berkhuijsen, E. M., Haslam, C. G. T., & Salter, C. J. 1971, A&A, 14, 252
Blaauw, A. 1964, ARA&A, 2, 213
Cernicharo, J., Bachiller, R., & Duvert, G. 1985, A&A, 149, 273
Colomb, F. R., Pflppel, W. G. L., & Heiles, C. 1980, A&AS, 40, 47
Condon, J. J., & Broderick, J. J. 1985, AJ, 90, 2540
Condon, J. J., Broderick, J. J., & Seielstad, G. A. 1989, AJ, 97, 1064
Désert, F. X., Bazell, D., & Boulanger, F. 1988, ApJ, 334, 815
Dwarakanath, K. S., & Shankar, U. 1990, J. Astrophys. Astron., 11, 323
Fiedler, R. L., Dennison, B., Johnston, K. J., Waltman, E., & Simon, R. 1994, ApJ, 430, 581
Gerazi, D. Y., Schmitz, M., & Mead, J. M. 1987, Catalog of Infrared Observations (NASA Ref. Pub. 1196), 597
Haslam, C. G. T., Salter, C. J., Stoffel, H., & Wilson, W. E. 1982, A&AS, 47, 1
Heiles, C., & Jenkins, E. B. 1976, A&A, 46, 333
Hu, E. M. 1981, ApJ, 248, 119
Lesh, J. R. 1969, AJ, 74, 891
McCray, R. 1987, in Physical Processes in Interstellar Clouds, ed. G. Morfill & R. Scholer (Dordrecht: Reidel), 95
Marscher, A. P., & Broderick, J. J. 1982, ApJ, 255, 11
———. 1985, ApJ, 290, 735
Marscher, A. P., Broderick, J. J., Padrielli, L., Bartel, N., & Romney, J. D. 1987, ApJ, 319, 456
Pauls, T., & Schwartz, P. R. 1989, in Lecture Notes in Physics, 331, The Physics and Chemistry of Interstellar Molecular Clouds, ed. G. Winnewisserr & J. T. Armstrong (Berlin: Springer), 225
Riley, J. M. 1989, MNRAS, 238, 1055
Romani, R. W. 1988, in Radiowave Scattering in the Interstellar Medium, ed. J. M. Cordes, B. J. Rickett, & D. C. Backer (AIP Conf. Proc. 174), 156
Sancisi, R., Goss, W. M., Anderson, C., Johansson, L. E. B., & Winnberg, A. 1974, A&A, 35, 445
Stark, A. A., Bally, J., Linke, R. A., & Heiles, C. 1981, unpublished
van Buren, D., & McCray, R. 1988, ApJ, 329, 93
Weaver, R., McCray, R., Castor, J., Shapiro, P., & Moore, R. 1977, ApJ, 218, 377
Wood, K. S., et al. 1984, ApJS, 56, 507